

P-type electrical, photoconductive, and anomalous ferromagnetic properties of Cu₂O nanowires

L. Liao,¹ B. Yan,¹ Y. F. Hao,² G. Z. Xing,¹ J. P. Liu,³ B. C. Zhao,¹ Z. X. Shen,¹ T. Wu,¹ L. Wang,¹ J. T. L. Thong,² C. M. Li,³ W. Huang,⁴ and T. Yu^{1,a)}

¹*Division of Physics and Applied Physics, School of Physical and Mathematical Sciences, Nanyang Technological University, Singapore 63737, Singapore*

²*Department of Electrical and Computer Engineering, National University of Singapore, Singapore 117576, Singapore*

³*School of Chemical and Biomedical Engineering and Center for Advanced Bionanosystems, Nanyang Technological University, Singapore 639798, Singapore*

⁴*Jiangsu Key Laboratory for Organic Electronics & Information Displays, Nanjing University of Posts and Telecommunications, 9 Wenyuan Road, Nanjing 210046, People's Republic of China*

(Received 27 December 2008; accepted 17 February 2009; published online 17 March 2009)

Cu₂O nanowires are synthesized by reduction of CuO nanowires with hydrogen gas. Strong green photoluminescence dominated by band-edge emission is observed. Field effect transistors fabricated from individual Cu₂O nanowires present high on-off ratio ($>10^6$) and high mobility (>95 cm²/V s). Furthermore, the device demonstrates a fast photoelectric response to blue illumination in air at room temperature. In addition, anomalous ferromagnetism appears in Cu₂O nanowires, which may originate from the defects in Cu₂O nanowires. This work shows the application potentials of the Cu₂O nanowires, especially in an electrical and photonic device.

© 2009 American Institute of Physics. [DOI: 10.1063/1.3097029]

Nanowires (NWs) of a high aspect ratio and a nanoscale diameter have attracted intensive interest owing to their exceptional properties and promising applications in many potential technologies. Up to now, many semiconductor NWs have been successfully applied in nanodevices, including field effect transistor (FETs),¹ nanolasers,² and nanogenerators.³

Cu₂O is a *p*-type semiconductor of cubic structure with a direct band gap of 2.17 eV.^{4,5} Its outstanding excitonic properties including a large exciton binding energy (~ 140 meV) have been the target of much research efforts during the past decades.⁴ Cu₂O layers on semiconductor and insulator substrates have exhibited interesting properties for field effect transistors,⁶ photovoltaic devices⁷ and photoelectrodes in high-efficiency photoelectrochemical cells.⁸ Recently, Cu₂O nanostructures including nanospheres,⁹ nanocubes,¹⁰ and NWs⁵ have been synthesized with a variety of techniques. So far, however, there have been few reports on the physical properties and the practical potential of the Cu₂O nanostructures, especially in electrical or photonic devices.

In this letter, we report that Cu₂O NWs could be conveniently synthesized by reduction in CuO NWs in hydrogen gas. Strong green photoluminescence (PL) and anomalous ferromagnetism were observed in Cu₂O NWs. We further fabricated FETs based on individual Cu₂O NWs. Compared with CuO NW FETs,¹¹ the Cu₂O NWs FETs show improved *p*-type transport performance with higher conductivity and higher mobility. In addition, the Cu₂O NW devices demonstrate a fast photoresponse to blue illumination in air at room temperature.

Experimentally, CuO NWs were synthesized by the oxidation Cu foil in atmosphere according to a previous work.¹² Afterwards, the as-grown CuO NWs were reduced in H₂/Ar 20% atmosphere at 200 °C for 1 h, and a red Cu₂O NWs film could be obtained. The microstructures and morphologies of the samples were characterized by x-ray diffraction (XRD) using a D8 Advanced diffractometer with Cu *K* α line and a JEOL 6700 FEG scanning electron microscope (SEM), respectively. The lattice images of Cu₂O NW were observed by a JEOL 2010F high-resolution transmission electron microscope (HRTEM). Magnetic behavior was measured using a Quantum Design Physical Property Measurement System in the temperature range of 5 to 350 K. The PL spectra were recorded by a WITEC CRM200 confocal system with 532 nm laser (spot size: 500 nm).

To fabricate single NW FETs, the Cu₂O NWs were removed by sonication from the substrates and subsequently dispersed in ethanol. The solution was dropped on SiO₂/*p*⁺-Si (i.e., 200 nm insulated SiO₂ film covering *p*⁺-Si substrate), and photoresist layer of polymethylmethacrylate was subsequently spun over the SiO₂/*p*⁺-Si substrate. Two electrical contact fingers together with their bonding pads were exposed by electron-beam lithography. After the development, a 100 nm thick Au film was deposited over the structure and followed by a lift-off process. The electrical transport properties were measured by Suss probe station with a Keithley 4200 SCS. Gate voltages were applied to the *p*⁺-Si substrate in standard global back-gate geometry. To characterize their photoresponse of current flowing through the Cu₂O NWs, Ar laser (488 nm) was used as light source.

A low-magnification SEM image [Fig. 1(a)] shows that the aligned Cu₂O NWs on the substrate are about 20–30 μ m in length and about 50–100 nm in diameter. Figure 1(b) gives the XRD pattern of Cu₂O NWs. Both Cu and Cu₂O phases are present. The peaks of Cu phase come from the Cu foil, which serves as both the substrate and the raw

^{a)} Author to whom correspondence should be addressed. Electronic mail: yuting@ntu.edu.sg. URL: www.ntu.edu.sg/home/yuting/. Tel.: +65-6316-7899.

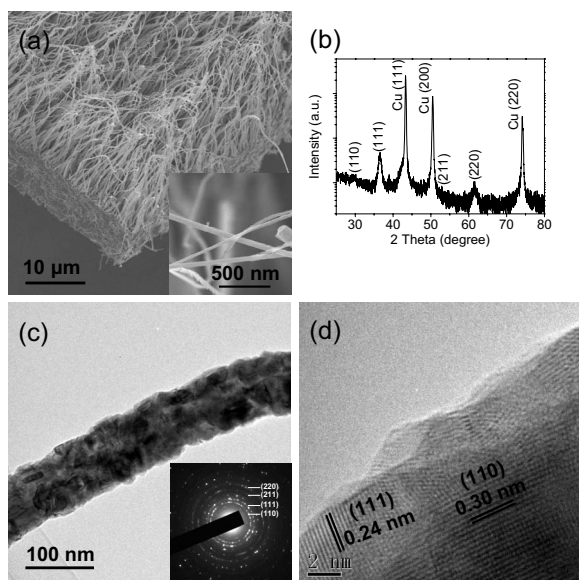


FIG. 1. (a) SEM image of Cu_2O NWs on Cu foils. Inset shows a high magnification SEM image, (b) XRD pattern of Cu_2O NWs on Cu foil, (c) TEM, and (d) HRTEM images of Cu_2O NWs; the inset of (c) shows the corresponding selected area electron diffraction pattern.

material source.¹³ A typical TEM image of the Cu_2O NWs is shown in Fig. 1(c). A selected area diffraction pattern of the NW [inset of Fig. 1(c)] reveals that the Cu_2O NW is polycrystalline. Figure 1(d) displays a HRTEM image, which shows interplanar spacings of 0.24 and 0.30 nm, consistent with the (111) and (110) lattices of cubic-phase Cu_2O .

Figure 2 shows PL spectrum of a single Cu_2O NW. The peak ~ 590 nm corresponds to the band edge of Cu_2O , which has a direct band gap of 2.17 eV.⁵ The inset (middle) of Fig. 2 is the PL image of a single Cu_2O NW with single spectrum integration time of half second, showing the homogeneous luminescence intensity. It was noted that the Cu_2O NWs present strong room temperature PL as demonstrated by the optical picture in the inset (right) of Fig. 2. This might indicate the high efficiency of photon-electron and/or exciton coupling in Cu_2O NWs.

In previous work, we reported an FET of CuO NW, which exhibits p -type conductive channel with field-effect mobility over $2\text{--}5\text{ cm}^2/\text{V s}$.¹¹ In this work, the Cu_2O NW is also used to as the conductive channel of the FET. An optical

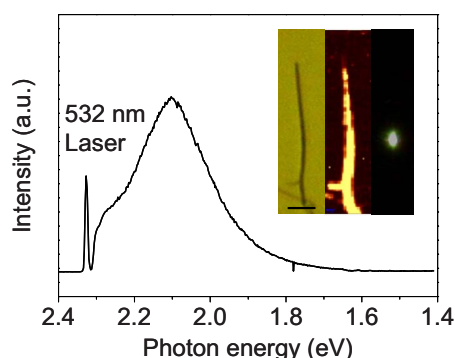


FIG. 2. (Color online) PL of a single Cu_2O NW, inset of (b) shows an optical (left) and PL (middle) images of the individual NW. The right inset is a large-view optical image of PL emission under illumination of a green laser. The bright spot shows the strong PL emission from Cu_2O NW. Scale bar=2 μm .

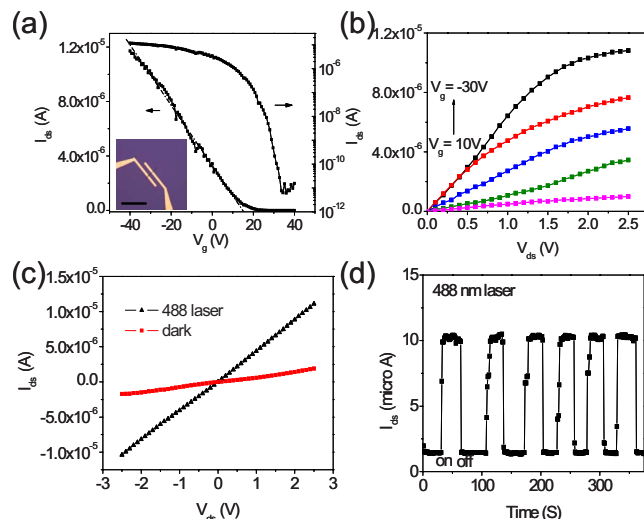


FIG. 3. (Color online) (a) $I_{ds}\text{-}V_g$ curve of single Cu_2O NW FET, inset shows optical image of a single Cu_2O NW FET, scale bar=20 μm . (b) $I_{ds}\text{-}V_{ds}$ curves of a single Cu_2O NW FET in the dark, and 488 nm laser illumination. (c) $I\text{-}V$ curves of a single Cu_2O NW in the dark, and 488 nm laser illumination. (d) Photoresponse of a Cu_2O NW, biased at 2.5 V, with 488 nm laser illumination.

microscope image of a single Cu_2O NW FET is shown in inset of Fig. 3(a). Figure 3(a) shows the $I_{ds}\text{-}V_g$ curve of single NW FET, which reveals that the on-off ratio is more than 10^6 . Figure 3(b) displays the $I_{ds}\text{-}V_{ds}$ curves of a typical Cu_2O NW FET. From the $I_{ds}\text{-}V_{ds}$ curves obtained under gate voltages (V_g) of -30 , -20 , -10 , 0 , and 10 V, it can be clearly seen that the conductance of the NW decreases as the gate potential increases, demonstrating that the Cu_2O NW is a p -type semiconductor. The field effect mobility (μ) in a typical cylindrical NW of a radius r can be calculated according to Ref. 11. The transconductance $g_m=dI/dV_g=0.22\text{ }\mu\text{S}$ can be extrapolated from the linear region (-40 V to 15V) of the $I_{ds}\text{-}V_g$ curve. Moreover, the mobility μ_e is $95\text{ cm}^2/\text{V s}$ at $V_g=0$ V, which is higher than that of CuO NW FET and similar to that of single phase Cu_2O epitaxial film.^{6,11}

Photogenerated carriers could significantly increase the conductivity when semiconductor materials are illuminated by high energy photons.¹⁴ Meanwhile, the large surface to volume ratio of semiconductor NWs is able to further enhance the sensitivity of the NW devices to light and even possibly leads to the realization of single photon detection.¹⁵ In this work, for the first time, the photoconductivity of Cu_2O NWs were investigated. Figure 3(c) shows $I\text{-}V$ characteristics of the Cu_2O NW, measured in the dark room and with blue (488 nm) laser illumination. The conductance of NW increased from 0.7 to 4.3 μS under blue laser illumination. Time-resolved measurements of photoresponse to 488 nm laser were conducted and the results are shown in Fig. 3(d). The “on” current and “off” current for each six cycle remain the same within the noise envelope, indicating the reversibility and stability of the Cu_2O NWs optical switches. The photoconductivity response time is less than three seconds.

Finally, we measured the magnetic properties of Cu_2O NWs. Figure 4(a) displays the magnetization versus magnetic field ($M\text{-}H$) curve of Cu_2O NWs at room temperature, and the diamagnetic signals from Cu substrate were subtracted. Interestingly, ferromagnetic hysteresis loops can be

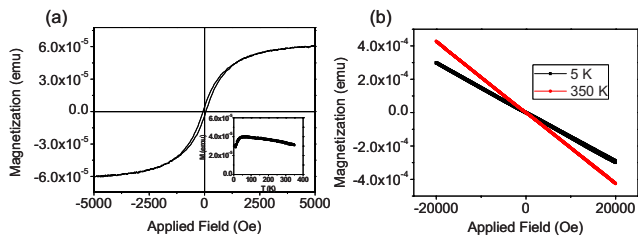


FIG. 4. (Color online) (a) M - H curve of Cu_2O NWs at room temperature; inset of (a) displays the M - T curve of Cu_2O NWs. (b) M - H curve of CuO NWs at 5 and 350 K.

clearly observed from the M - H curves with a coercive field of ~ 60 Oe. The temperature dependence of magnetization (M - T) of the Cu_2O NWs in the temperature range from 5 to 350 K under zero-field cooled modes at 500 Oe is shown in the inset of Fig. 4(a). At all temperatures, the Cu_2O NWs always exhibit weak ferromagnetic behavior. Recently, Wang *et al.*¹⁶ also reported a similar phenomenon. However, bulk Cu_2O is well known as an antiferromagnetic material.¹⁷ To confirm that the ferromagnetism originates from Cu_2O NW rather than unintentionally introduced contaminations, such as Fe, Co, etc., we also measured the M - H curves of other Cu_2O NWs samples and compared the as-grown CuO NWs. All Cu_2O NWs consistently samples show ferromagnetism at room temperature. As shown in Fig. 2(b), only diamagnetism curves are observed in CuO NWs, which comes from the copper substrate.¹⁸ We propose that the ferromagnetism originates from the defects in Cu_2O NWs.^{16,19} In our experiment, the Cu_2O NW is polycrystalline, so there are many defects, which prefer to reside on the surface and the grain boundary. The origin of magnetism may not result from the Cu $3d$ electrons but instead from the unpaired $2p$ electrons of O atoms in the immediate vicinity of the cation vacancies. We will continue to research the ferromagnetism of Cu_2O NWs and look for the relative mechanism of Cu_2O NWs in the future.

In conclusion, we report on the synthesis, optical, electrical, and magnetic properties of polycrystalline Cu_2O NWs.

PL spectra of Cu_2O NWs were measured, showing that the optical band gap of Cu_2O NWs is around 2.17 eV. Electrical measurements of Cu_2O NWs FETs demonstrated their high performance p -type conduction with large on-off ratio ($>10^6$), and high mobility (~ 95 $\text{cm}^2/\text{V s}$). Under blue laser irradiation, the conductance of Cu_2O NWs increased with a time constant of several seconds. Anomalous ferromagnetism was also observed in such polycrystalline Cu_2O NWs and attributed to defects.

L. Liao acknowledges the support in this work by the Singapore Millennium Foundation 2008 fellowship.

- ¹X. F. Duan, Y. Huang, Y. Cui, J. F. Wang, and C. M. Lieber, *Nature (London)* **409**, 66 (2001).
- ²M. H. Huang, S. Mao, H. Feick, H. Q. Yan, Y. Y. Wu, H. Kind, E. Weber, R. Russo, and P. D. Yang, *Science* **292**, 1897 (2001).
- ³Z. L. Wang and J. H. Song, *Science* **312**, 242 (2006).
- ⁴L. F. Gou and C. J. Murphy, *Nano Lett.* **3**, 231 (2003).
- ⁵W. Z. Wang, G. H. Wang, X. S. Wang, Y. J. Zhan, Y. K. Liu, and C. L. Zheng, *Adv. Mater. (Weinheim, Ger.)* **14**, 67 (2002).
- ⁶K. Matsuzaki, K. Nomura, H. Yanagi, T. Kamiya, M. Hirano, and H. Hosono, *Appl. Phys. Lett.* **93**, 202107 (2008).
- ⁷A. Mittiga, E. Salza, F. Sarto, M. Tucci, and R. Vasanthi, *Appl. Phys. Lett.* **88**, 163502 (2006).
- ⁸P. E. de Jongh, D. Vanmaekelbergh, and J. J. Kelly, *J. Electrochem. Soc.* **147**, 486 (2000).
- ⁹Y. Chang, J. J. Teo, and H. C. Zeng, *Langmuir* **21**, 1074 (2005).
- ¹⁰J. J. Teo, Y. Chang, and H. C. Zeng, *Langmuir* **22**, 7369 (2006).
- ¹¹L. Liao, Z. Zhang, B. Yan, Z. Zheng, Q. L. Bao, T. Wu, C. M. Li, Z. X. Shen, J. X. Zhang, H. Gong, J. C. Li, and T. Yu, *Nanotechnology* **20**, 085203 (2009).
- ¹²T. Yu, X. Zhao, Z. X. Shen, Y. H. Wu, and W. H. Su, *J. Cryst. Growth* **268**, 590 (2004).
- ¹³Y. W. Zhu, T. Yu, F. C. Cheong, X. J. Xui, C. T. Lim, V. B. C. Tan, J. T. L. Thong, and C. H. Sow, *Nanotechnology* **16**, 88 (2005).
- ¹⁴S. M. Sze, *Physics of Semiconductor Device* (Wiley, New York, 1981).
- ¹⁵O. Hayden, R. Agarwal, and C. M. Lieber, *Nature Mater.* **5**, 352 (2006).
- ¹⁶Q. Wang, Q. Sun, G. Chen, Y. Kawazoe, and P. Jena, *Phys. Rev. B* **77**, 205411 (2008).
- ¹⁷E. Manousakis, *Rev. Mod. Phys.* **63**, 1 (1991).
- ¹⁸H. M. Zeyada, *Phys. Scr.* **46**, 538 (1992).
- ¹⁹C. P. Chen, L. He, L. Lai, H. Zhang, J. Lu, L. Guo, and Y. D. Li, arXiv:0812.2079v1.